JOC Article
pubs.acs.org/joc

On the Causes of Potential Inversion in 1,2,4,5-Tetrakis(amino)benzenes

Christopher J. Adams,*,† Rosenildo C. da Costa,† Ruth Edge,‡ Dennis H. Evans,§ and Matthew F. Hood†

†*School of Chemistry, University of Bristol, Bristol BS8 1TS, U.K.,* ‡*EPSRC National EPR Service, School of Chemistry, University of Manchester, Oxford Road, Manchester M13 9PL, U.K., and* §*Department of Chemistry, Purdue University, 560 Oval Drive, West Lafayette, Indiana 47907-2084*

chcja@bris.ac.uk

Received November 11, 2009

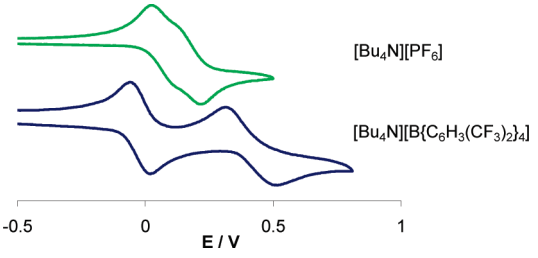

Three 3,6-difluoro-1,2,4,5-tetrakis(amino)benzene compounds, bearing dimethylamino (**1**), piperidin-1-yl (**3**), or morpholin-1-yl (**5**) substituents, have been synthesized and subsequently defluorinated to give the corresponding 1,2,4,5-tetrakis(amino)benzene compounds **2**, **4**, and **6**; the crystal structures of compounds **1**, **4**, and **6** have been obtained. Cyclic voltammetry shows that all six compounds will lose two electrons to form dications, and the use of suitable oxidizing agents has allowed isolation and crystallographic characterization of the dications $\mathbf{2}^{2+}$ and $\mathbf{6}^{2+}$ (as $[PF_6]_2$ salts) and $\mathbf{4}^{2+}$ (as a $[I_5][I_3]$ salt). The separation ΔE between the loss of the first electron and the second varies between compounds, from 0.23 V in **1** to 0.01 V in **6**. Eletrochemical studies involving the use of the noncoordinating electrolyte $[Bu_4N][B\{C_6H_3(CF_3)_2\}_4]$ show that it is possible to increase this separation, stabilizing the intermediate monocationic phase, and this has allowed the isolation and crystallographic characterization of the radical salts $\mathbf{2}[B\{C_6H_3(CF_3)_2\}_4]$ and $\mathbf{4}[B\{C_6H_3(CF_3)_2\}_4]$, the first radical cations of this family to be isolated. DFT studies of the ion pairing between oxidized forms of **1** and **2** and anions imply that the location of the ion pairing is different in the two species.

Introduction

It has been known for many years that aromatic compounds bearing amino substituents are very electron-rich systems that may be used as electron donors. The archetypal system is *N*,*N*,*N*′,*N*′-tetramethyl-1,4-diaminobenzene, whose radical cation is generated from the neutral species at an oxidation potential of 0.17 V vs SCE and which is colloquially known as "Wurster's blue" after its discoverer and its color. Although oxidation involves loss of the aromaticity associated with the neutral molecule, generation of the quinonoidal mono- and dications places the nonbonding nitrogen lone-pair electrons into bonding orbitals and is thus relatively easy to do.[1]

It stands to reason that the addition of further amino groups to such a system would render it more electron-rich and more easily oxidized, and that, therefore, in situations where an electron donor was required, such compounds might fulfill this role (as indeed *N*,*N*,*N*′,*N*′-tetramethyl-1,4-diaminobenzene sometimes does). This was demonstrated by Staab and co-workers in 1986, when they reported the synthesis and characterization of 1,2,4,5-tetrakis(dimethylamino)benzene (**2**).[2] In contrast to *N*,*N*,*N*′,*N*′-tetramethyl-1,4-diaminobenzene, this compound did not form a radical cation but underwent a *two*-electron oxidation at −0.03 V vs SCE in acetonitrile. The resulting dication $\mathbf{2}^{2+}$ has 12 π-electrons, which would render it antiaromatic were they all conjugated, so it undergoes a structural distortion to create a molecule that effectively consists of two 6 π-electron 1,3-bis(dimethylamino)allyl cations, which are linked by single

(1) Michaelis, L. *Chem. Rev.* **1935**, *16*, 243–286.

(2) Elbl, K.; Krieger, C.; Staab, H. A. *Angew. Chem., Int. Ed. Engl.* **1986**, *25*, 1023–1024.

Published on Web 01/14/2010 DOI: 10.1021/jo902411b

SCHEME 1[a]

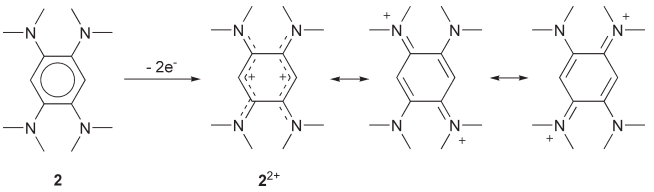

[a]Two-electron oxidation of 14 π-electron 1,2,4,5-tetrakis(amino)-benzene compounds such as **2** generates dications composed of two monocationic 1,3-diaminoallyl subunits, each containing 6 π-electrons, linked by two carbon−carbon single bonds. To emphasise the similarities to the *N*,*N*,*N*′,*N*′-tetramethyl-1,4-diaminobenzene dication, the dication $\mathbf{2}^{2+}$ may be drawn in two quinonoidal forms each with two localized positive charges.

SCHEME 2. Azophenine-Type Systems (Left) Become Isoelectronic with $\mathbf{2}^{2+}$ upon Diprotonation

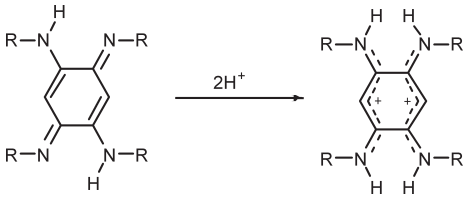

bonds at the 1 and 3 positions so that there is no through-conjugation (Scheme 1). The theoretical description of the bonding in $\mathbf{2}^{2+}$ was deduced by Dähne and Leupold over 40 years ago[3] and more recently elaborated upon by Braunstein and co-workers,[4] who synthesized some azophenine-type systems with alkyl substituents.[5] These complexes are readily diprotonated, at which point they are isoelectronic with $\mathbf{2}^{2+}$ (Scheme 2); $\mathbf{2}^{2+}$ is also isoelectronic with the family of 2,5-diamino-*p*-benzoquinones, and the whole family may be classified as coupled trimethines.[3]

Given the use of *N*,*N*,*N*′,*N*′-tetramethyl-1,4-diaminobenzene and similar 1,4-diamines as electron donors, it would seem logical to use the more electron-releasing tetrakis-(amino) systems in the same way, but this has not happened. The reason for this is that there has been no generally applicable high yielding synthetic route to these compounds−**2** was made in 27% yield by a route which cannot be extended to derivatives containing substituents other than methyl groups. However, modern synthetic methodologies have provided two potential routes to such compounds. The first is the well-known Buchwald−Hartwig amination reaction, which involves the palladium-catalyzed coupling of an aryl halide with an amine. The second involves the protodefluorination of 1,2,4,5-tetrakis(amino)-3,6-difluorobenzene compounds,[6] which are simply 1,2,4,5-tetrakis(amino)benzene compounds in which the hydrogen atoms on the central benzene ring have been replaced by fluorine atoms. This is a readily prepared class of compound, being synthesized by the nucleophilic attack of lithium amides

SCHEME 3. Buchwald−Hartwig Synthesis of 6

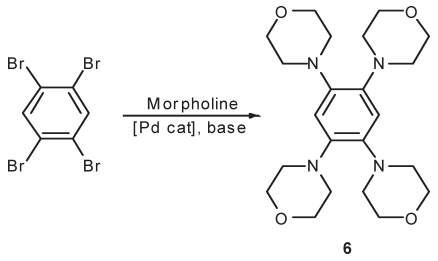

on hexafluorobenzene.[7] We therefore set out to synthesize some of these compounds and to investigate their properties to see whether they might be of use as electron donors.

Results and Discussion

Synthesis. The Buchwald−Hartwig coupling of 1,2,4,5-tetrabromobenzene with a variety of primary amines gives tetrakis(secondary amines) in good yields. This was first reported by Wenderski[8] with 2,6-dimethyl- and 2,6-diisopropylanilines as the amines and greatly expanded upon by Bielawski,[9] who extended the range of substrates to include sterically bulky alkylamines. However, the literature contains only the synthesis of a single 1,2,4,5-tetrakis(tertiary amino)benzene compound, in which 1,2,4,5-tetrabromobenzene was coupled with morpholine to yield the corresponding tetrakis(morpholin-1-yl) compound **6** (Scheme 3).[10]

In order to extend the scope of this reaction, we examined the reactions of 1,2,4,5-tetrabromo- and 1,2,4,5-tetraiodobenzene with a variety of secondary amines in the presence of a range of different catalysts and under a variety of conditions without being able to find another system which effectively produces the desired product. The only successful coupling reactions used morpholine as the amine to produce the aforementioned compound **6**; even other cyclic secondary amines such as thiomorpholine and piperidine did not work. Generally, byproducts were observed that had resulted from partial protodehalogenation of the benzene ring, and which were thus di- or triaminated.

Given the failure of the palladium-catalyzed methodology, we were required to use the lithiation and protodefluorination pathway outlined in Scheme 4, which was developed by Sorokin and co-workers to prepare a variety of such compounds with piperidine, pyrrolidine, dimethylamine, and dibutylamine as substrates. The 3,6-difluorinated compounds may be converted to the corresponding protio derivatives by reaction with sodium biphenylide;[6] using this reaction sequence, we have synthesized the 1,4-difluorotetrakis(amino)benzene compounds **1**, **3**, and **5** and subsequently defluorinated them to yield the corresponding compounds **2**, **4**, and **6** (Scheme 4).

Electrochemical Studies. Our primary motivation for synthesizing these compounds was to investigate the effect that the various substituents and substitution patterns would have on their electrochemical properties. Cyclic voltammetry

(3) Dähne, S.; Leupold, D. *Angew. Chem., Int. Ed. Engl.* **1966**, *5*, 984–993.
(4) Braunstein, P.; Siri, O.; Taquet, J.-P.; Rohmer, M.-M.; Bénard, M.; Welter, R. *J. Am. Chem. Soc.* **2003**, *125*, 12246–12256.
(5) Siri, O.; Braunstein, P.; Rohmer, M.-M.; Bénard, M.; Welter, R. *J. Am. Chem. Soc.* **2003**, *125*, 13793–13803.
(6) Sorokin, V. I.; Ozeryanskii, V. A.; Borodkin, G. S. *Synthesis* **2006**, 97–102.
(7) Sorokin, V. I.; Ozeryanskii, V. A.; Borodkin, G. S.; Chernyshev, A. V.; Muir, M.; Baker, J. *Z. Naturforsch.* **2006**, *61b*, 615–625.
(8) Wenderski, T.; Light, K. M.; Ogrin, D.; Bott, S. G.; Harlan, C. J. *Tetrahedron Lett.* **2004**, *45*, 6851–6853.
(9) Khramov, D. M.; Boydston, A. J.; Bielawski, C. W. *Org. Lett.* **2006**, *8*, 1831–1834.
(10) Witulski, B.; Senft, S.; Thum, A. *Synlett* **1998**, 504–506.

SCHEME 4. Synthesis of 1−6 from C_6F_6

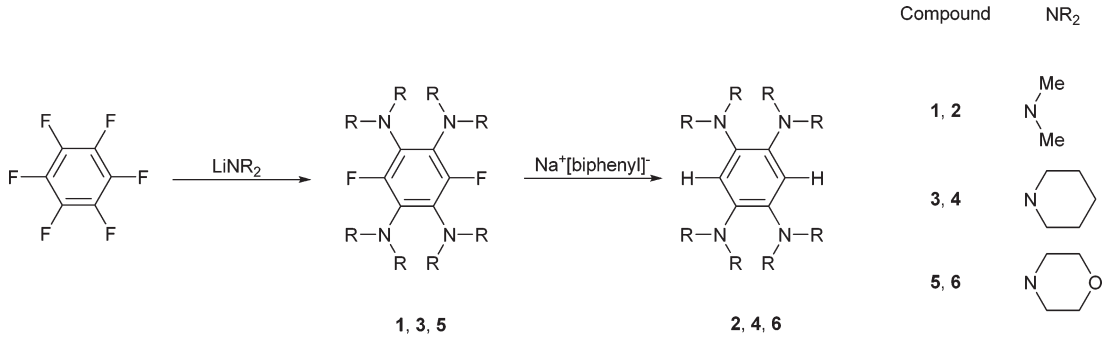

TABLE 1. First and Second Oxidation Potentials (V vs SCE, CH_2Cl_2, 0.1 M $[Bu_4N][PF_6]$) of All Compounds[a]

		$E°_1$, $E°_2$	ΔE		$E°_1$, $E°_2$	ΔE
1	methyl	0.430, 0.660	0.230	**2**	0.063, 0.171	0.108
3	piperid-1-yl	0.475, 0.625	0.150	**4**	0.110, 0.265	0.155
5	morpholin-1-yl	0.685, 0.745	0.060	**6**	0.445, 0.455	0.010

[a] $E°$ values were obtained by digital simulation of the experimental data (see the Supporting Information for further details).

showed that all of them underwent the reversible loss of two electrons, with varying degrees of separation ΔE ($= E°_2 - E°_1$) between the two processes (Table 1).

The values show the expected trends. The fluorine atoms move the oxidations of **1**, **3**, and **5** to more positive potentials as compared to their protio analogues, and the oxidation potentials of **5** and **6**, with the less electron-donating morpholinyl substituents, are 0.3−0.4 V higher than those of the methyl and piperidinyl compounds. The most interesting feature lies in the values of ΔE, which vary from compound to compound, and which vary from two one-electron processes in **1** to a single two-electron process in **6**.

The phenomenon in which ΔE is reduced is known as *potential compression*, and when $\Delta E \leq 0$, *potential inversion* is seen and both electrons are apparently lost at once.[11] One of the factors that can cause potential compression and inversion is a significant geometric change following loss of the first electron. Normally, it is harder to remove a second electron from a compound than the first because of the increased electrostatic attraction between a cation and an electron compared to the neutral species and the electron; this is equivalent to saying that the SOMO is stabilized in the cation compared to its energy as the HOMO in the neutral compound. However, if the geometric change undergone following the first oxidation causes a change in the composition and energy of the molecular orbitals such that stabilization of the SOMO of the cation is less than expected, then the system will lose the second electron at a potential near that at which the first is lost; should the SOMO actually be destabilized (relative to the HOMO of the neutral compound), then the second electron will be easier to remove than the first and potential inversion will result. One reason for the smaller value of ΔE for **2** than **1** could therefore be that **2** undergoes a larger geometric change than **1** on undergoing one-electron oxidation. This hypothesis was tested by measuring the EPR spectrum of the radical cation $\mathbf{1}^+$ (Figure 1), which revealed coupling constants to all four nitrogen atoms (a = 3.50 G), both fluorine atoms (4.30 G) (there are many examples of pairs of organic radicals which differ only in the substitution of hydrogen for fluorine, and often the ratio $|a_F|/|a_H|$ of the coupling constants is around 2.0−3.0; however, these are exclusively *anionic* radicals; in the case of **1** and **2**, the ratio is either 5 or 10 (a_H for **1** was either 0.42 or 0.84 G), and we have been unable to find any other similar such *cationic* pairs for comparison; see ref 12 for further discussion) and all 24 hydrogen atoms of the methyl groups (3.50 G). The similarity of the values to those reported for the radical $\mathbf{2}^+$, which were a(N) = 3.57 G and a(Me) = 3.13 G,[12] implies that the unpaired electron is distributed similarly in both $\mathbf{1}^+$ and $\mathbf{2}^+$.

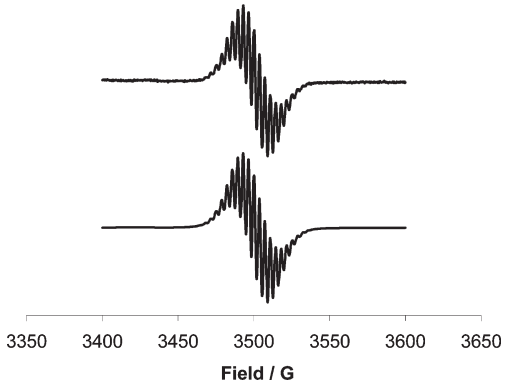

FIGURE 1. Simulated (bottom) and experimental (top) EPR spectra of $\mathbf{1}^+$.

Therefore, we conclude that both radicals have similar electronic structures (and, by extension, geometric structures), and that the difference in ΔE of **1** and **2** is not due to them undergoing radically different structural changes. We were unable to obtain well-resolved EPR spectra for $\mathbf{3}^+$ or $\mathbf{5}^+$.

Another factor that may influence ΔE is ion pairing between the cationic species generated upon oxidation and the anion of the supporting electrolyte. The work, in particular, of Geiger and co-workers has demonstrated how changing from electrolytes containing anions such as $[ClO_4]^-$ and $[PF_6]^-$ to those with much larger noncoordinating anions such as $[B(C_6F_5)_4]^-$ and $[B\{C_6H_3(CF_3)_2\}_4]^-$ can dramatically increase ΔE, separating two-electron processes into two one-electron processes.[13] This occurs because ion pairing has an important effect in stabilizing charged species.

(11) Evans, D. H. *Chem. Rev.* **2008**, *108*, 2113–2144.

(12) Elbl-Weiser, K.; Neugebauer, F. A.; Staab, H. A. *Tetrahedron Lett.* **1989**, *30*, 6161–6164.

(13) Nafady, A.; Chin, T. T.; Geiger, W. E. *Organometallics* **2006**, *25*, 1654–1663.

TABLE 2. Oxidation Potentials for 2 (V vs SCE) with Different Solvents and Electrolytes $[Bu_4N]^+A^-$

solvent	CH_2Cl_2			CH_3CN		
entry in Figure 2	a	b	c	d	e	f
A^-	$[B\{C_6H_3(CF_3)_2\}_4]^-$	$[PF_6]^-$	$[ClO_4]^-$	$[B\{C_6H_3(CF_3)_2\}_4]^-$	$[PF_6]^-$	$[ClO_4]^-$
E°_1	−0.010	0.070	0.120	0.042	0.065	0.042
E°_2	0.408	0.171	0.165	0.053	0.070	0.050
ΔE	0.418	0.101	0.045	0.011	0.005	0.008

The instability of the monocation in systems that display potential inversion can be quantified by using the free energy of disproportionation, $\Delta_{disp}G$, associated with the reaction $2B^+ \rightarrow B + B^{2+}$, where B is the analyte:

$$\Delta_{disp}G = \Delta_f G_B + \Delta_f G_{B^{2+}} - 2\Delta_f G_{B^+} = F\Delta E$$

Where no potential inversion is displayed, ΔE (and thus $\Delta_{disp}G$) is positive and the reaction stays on the left-hand side; the monocation is stable. When there is potential inversion, both ΔE and $\Delta_{disp}G$ are negative, and the system will spontaneously form dications. The electrostatic interaction between an electrolytic anion and an analyte cation has the effect of making $\Delta_f G$ more negative (in other words, the free energy of formation of the ion pair is more negative than that of the individual ions because of the electrostatic interaction between them), and this effect will be greater (because of the larger electrostatic effects) for the interaction of a dication with an anion than for a monocation with an anion. Thus, if the effect of ion pairing on $\Delta_f G_{B^{2+}}$ is to make it a great deal more negative than $\Delta_f G_{B^+}$, then this can render $\Delta_{disp}G$ negative and cause potential inversion.

In order to test whether this was the case, we studied the electrochemistry of **2** in CH_2Cl_2 and CH_3CN solutions with different supporting electrolytes (Table 2 and Figure 2). This showed that, in dichloromethane, when $[Bu_4N][ClO_4]$ or $[Bu_4N][PF_6]$ was used, two closely spaced processes were observed (ΔE = 0.045 or 0.101 V), but when $[Bu_4N][B\{C_6H_3(CF_3)_2\}_4]$ was used, two separate processes were observed (ΔE = 0.418 V). ESR measurements on the species generated following the first process confirmed it to be the radical cation $\mathbf{2}^+$ because it had identical coupling constants to those reported previously. In acetonitrile, no matter which electrolyte was used, essentially only one process was observed (ΔE < 0.011 V). The electrochemical reversibility of the processes was dependent somewhat upon the scan speed and the nature of the working electrode; the second wave showed much better reversibility at a glassy carbon (as opposed to a platinum) electrode and at slower scan speeds (50 rather than 500 mV/s). The lower electrochemical reversibility of the second oxidation compared to the first may be caused by a larger structural change associated with the second process than the first.

These results clearly indicate that in dichloromethane ion pairing has a large effect on the electrochemistry of **2**, with the increased ion pairing in the presence of $[PF_6]^-$ and $[ClO_4]^-$ resulting in a potential compression which is removed by the use of the noncoordinating electrolyte. The ordering of ΔE with the three electrolytes studied ($[ClO_4]^-$ < $[PF_6]^-$ < $[B\{C_6H_3(CF_3)_2\}_4]^-$) mirrors that found for the inorganic system $[Rh_2(TM4)_4]^{2+}$ (TM4 = 2,5-diisocyano-2,5-dimethylhexane)[14] and also confirms the fact that $[ClO_4]^-$ tends to cause a slightly smaller value of ΔE than $[PF_6]^-$ in systems with planar organic cationic π-radicals.[15] $[ClO_4]^-$ is slightly smaller than $[PF_6]^-$ (ionic radii of 0.290 and 0.301 nm, respectively) which may allow better ion pairing.

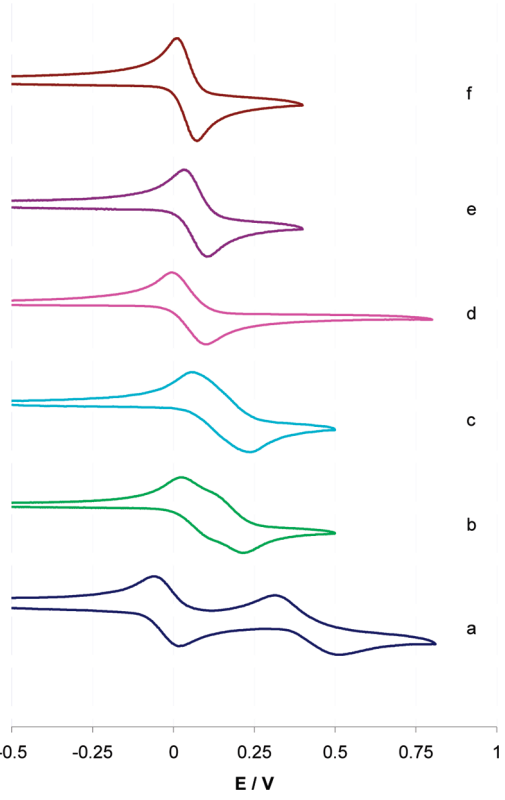

FIGURE 2. Oxidations of **2** at 50 mV s^{-1} in different combinations of solvent and electrolyte: (a) CH_2Cl_2, $[Bu_4N][B\{C_6H_3(CF_3)_2\}_4]$; (b) CH_2Cl_2, $[Bu_4N][PF_6]$; (c) CH_2Cl_2, $[Bu_4N][ClO_4]$; (d) MeCN, $[Bu_4N][B\{C_6H_3(CF_3)_2\}_4]$; (e) MeCN, $[Bu_4N][PF_6]$; (f) MeCN, $[Bu_4N][ClO_4]$.

In acetonitrile, all three electrolytes give little potential separation. This is consistent with the findings of Barrière and Geiger,[16] who demonstrated that in solvents of high polarity such as acetonitrile with medium or large electrolyte anions (such as $[PF_6]^-$ or $[B\{C_6H_3(CF_3)_2\}_4]^-$) the dominant effect on ΔE was the solvation of the cationic products of electrolysis. Under these circumstances, varying the anion has little effect on ΔE. They also found that with medium-sized electrolyte anions (including $[PF_6]^-$ and $[ClO_4]^-$) the choice of solvent has relatively little effect upon ΔE, again consistent with the data in Table 2, where the change in ΔE upon moving from CH_2Cl_2 to MeCN is 0.1 V or less for $[PF_6]^-$ and $[ClO_4]^-$ but more than 0.4 V for $[B\{C_6H_3(CF_3)_2\}_4]^-$.

(14) Hill, M. G.; Lamanna, W. M.; Mann, K. R. *Inorg. Chem.* **1991**, *30*, 4687–4690.

(15) Bancroft, E. E.; Pemberton, J. E.; Blount, H. N. *J. Phys. Chem.* **1980**, *84*, 2557–2560.

(16) Barrière, F.; Geiger, W. E. *J. Am .Chem. Soc* **2006**, *128*, 3980–3989.

TABLE 3. Selected Bond Lengths (Å) and Torsion Angles (°) for 1, 4, and 6 (Σ(N1) = Sum of the Three Bonding Angles at N1, etc.)

	1	4	6
C(1)−N(1)	1.4267(15)	1.4340(13)	1.425(4)
C(3)−N(2)	1.4158(15)	1.4266(13)	1.432(4)
C(1)−C(2)	1.3899(17)	1.3976(14)	1.399(4)
C(2)−C(3)	1.3950(17)	1.4005(14)	1.401(4)
C(1)-C(3A)	1.4110(16)	1.4141(14)	1.415(4)
Σ(N1)	342.8	339.6	342.7
Σ(N2)	347.0	340.1	339.6
C(2)−C(1)−C(3)−C(2)	1.54	1.15	0.66

Assuming that the geometric change experienced by **2** is the same in all solvents, we can therefore say first that in dichloromethane the potential compression is caused not by the geometric change but by ion pairing (because it is removed by the use of the noncoordinating anion), and second that in acetonitrile it is caused by cation−solvent interactions (because it is present even in the presence of the noncoordinating anion, and there is expected to be little ion pairing in this medium).

Structural Studies. Having established that in dichloromethane the reason for the potential compression for **2**, **4**, and **6** is indeed ion pairing between electrolyte anion and analyte cation, we reasoned that it might be possible to isolate their radical cations by using an oxidant such as [Fc][$B\{C_6H_3(CF_3)_2\}_4$] (Fc = ferrocenium), which would transfer the noncoordinating anion, whereas the dications might be obtained with [Fc][PF_6]. This was indeed the case, and crystals of the radical cations $\mathbf{2}^+$ and $\mathbf{4}^+$, as [$B\{C_6H_3(CF_3)_2\}_4$] salts, and the dications $\mathbf{2}^{2+}$ and $\mathbf{6}^{2+}$ (as $[PF_6]_2$ salts) and $\mathbf{4}^{2+}$ (as a $[I_5][I_3]$ salt) were isolated and studied by X-ray diffraction. The structures of the neutral compounds **1**, **4**, and **6** were also obtained for the purposes of comparison. We were unable to isolate oxidized versions of the fluorinated compounds **1**, **3**, and **5**; mass spectra suggested that decomposition involving defluorination was occurring following chemical oxidation. We note that the structure of $\mathbf{2}^{2+}$ as a mixed triiodide−iodide salt was reported by Staab and coworkers in their original communication.[2]

The neutral compounds **1**, **4**, and **6** all crystallized lying across a crystallographic inversion center and therefore have one-half of a molecule in the asymmetric unit, and there are no significant differences between the metrics of the fluorinated compound **1** and the nonfluorinated compounds **4** and **6** (Table 3). In all three compounds, within the aromatic central ring, the C−C distances C(1)−C(2) and C(2)−C(3) are 1.39−1.40 Å in length and the distance C(1)−C(3A) between the two halves of the system is marginally longer at 1.41 Å, but the differences are small. The sum of the angles at the nitrogen atoms, indicating the degree of pyramidalization and thus the hybridization (for a perfect sp^3 atom, this would be 328.5°), varies between 339 and 347°, with **1** having the greater values. The torsion angle C(2)−C(1)−C(3A)−C(2A) which indicates the planarity of the ring varies between 0 and 2°. Essentially, the systems are typical aminobenzenes, and the structure of **1** is shown in Figure 3 as an example.

The structures of the dications $\mathbf{2}^{2+}$, $\mathbf{4}^{2+}$, and $\mathbf{6}^{2+}$ are radically different to the neutral species. Two-electron oxidation creates a system with 12 π-electrons, which would be antiaromatic were they all conjugated. There is therefore a structural distortion which prevents this happening, which is

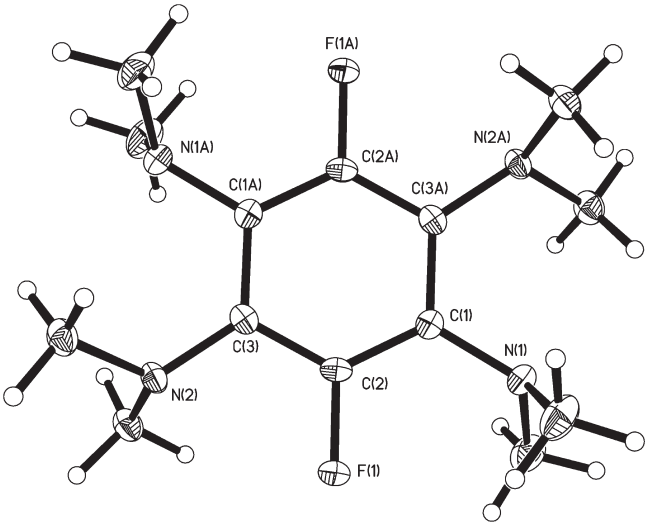

FIGURE 3. Molecular structure of **1** (50% probability ellipsoids). The same numbering scheme has also been used for **4** and **6**.

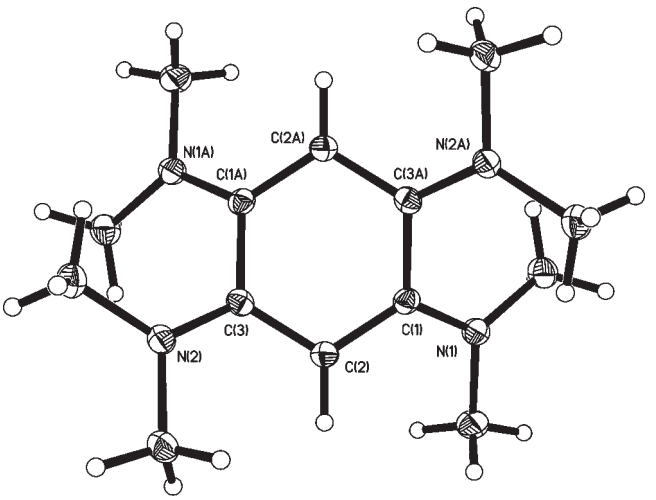

FIGURE 4. ORTEP plot (50% probability ellipsoids) of the cation $\mathbf{2}^{2+}$ in the structure of [**2**][$PF_6]_2$, showing the close contact between *endo*-methyl groups.

a separation of the molecule into what is effectively two 6 π-electron 1,3-diaminoallyl cyanine cations (Scheme 1). These are linked by two C−C single bonds which are long enough to prevent the π-systems overlapping, and the two halves of the molecule are also mutually twisted, again so that there is no effective overlap of the π-electron clouds on each side.

The cation $\mathbf{2}^{2+}$ (Figure 4) lies on a crystallographic center of symmetry. The C(1)−C(3A) bond which joins the two halves of the ring is now 1.51 Å long, an increase of 0.1 Å when compared to the neutral compounds. The carbon−nitrogen distances have decreased from about 1.42 Å in the neutral compounds to about 1.32 Å, consistent with the bond order increasing from 1 in the neutral compounds to 1.5 in the dications, while the allylic C−C distances along the sides of the central ring are largely unchanged; the C−C bond order in a 1,3-diaminoallyl cation is approximately the same as in a benzene ring, so there is little change. The sums of the three bond angles at the nitrogen atoms are 359°, indicating sp^2 hybridization, and the ring twist (Figure 5) as indicated

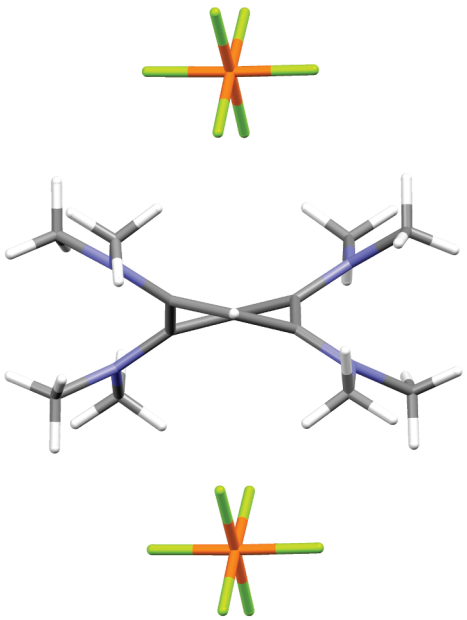

FIGURE 5. Side view of [**2**][PF]$_2$, showing the twisting of the cation and the location of the anions.

by the torsion angles is between 40 and 50°. There is a very short contact (carbon−carbon distance of 3.07 Å) between the *endo*-methyl groups of neighboring NMe_2 substituents; in the neutral species, these would be twisted out of the plane of the benzene ring, minimizing such interactions (see Figure 3), but in the dication, the requirement for conjugation of the nitrogen lone pair with the central ring prevents this. The radius of a methyl group is about 2 Å,[17] but it is not perfectly spherical, and interleaving of the hydrogen atoms in $\mathbf{2}^{2+}$ allows the short contact. Similar behavior, both in the distortion of the aromatic framework and the close methyl−methyl contacts, is seen upon oxidizing tetrakis(dimethylamino)-*p*-benzoquinone[17] and hexakis(dimethylamino)benzene.[18]

The structures of $\mathbf{4}^{2+}$ and $\mathbf{6}^{2+}$ show similar metrics to that of $\mathbf{2}^{2+}$, although in these cases, the cations are not on centers of symmetry so there are more independent values (Table 4). Interestingly, in both of these cases, there is some evidence of bond-length alternation (the core structure of $\mathbf{6}^{2+}$ is shown in Figure 6 as an example), with each diaminoallyl subunit having one short and one long C−C distance (1.38 and 1.42 Å, respectively), and though both C−N distances are shorter than in the neutral compound, one is longer than the other (1.30−1.33 vs 1.34−1.35 Å). The overall implication is that one of the quinonoid resonance forms shown in Figure 1 is making a greater contribution to the structure than the other. This is probably due to steric effects, the alternant bonding allowing a greater distance between neighboring piperidyl or morpholinyl termini than the delocalized bonding would.

The structures of the radical cations $\mathbf{2}^{+}$ (Figure 7) and $\mathbf{4}^{+}$ are interesting (Table 5), in that although the structures of several doubly oxidized polyaminobenzenes are known there are apparently no published structures of singly oxidized

(17) Bock, H.; Ruppert, K.; Näther, C.; Havlas, Z. *Angew. Chem., Int. Ed. Engl.* **1991**, *30*, 1180–1183.
(18) Speiser, B.; Würde, M.; Maichle-Mössmer, C. *Chem.—Eur. J.* **1998**, *4*, 222–233.

TABLE 4. Selected Bond Lengths (Å) and Angles (°) for 2[PF$_6$]$_2$, 4[I$_3$][I$_5$]·I$_2$, and 6[PF$_6$]$_2$ (Σ(N1) = Sum of the Three Bonding Angles at N1, *etc.*)

	2[PF$_6$]$_2$	**4**[I$_3$][I$_5$]·I$_2$	**6**[PF$_6$]$_2$
C(1)−N(1)	1.3219(19)	1.347(5)	1.341(4)
C(3)−N(2)	1.3192(19)	1.320(5)	1.332(3)
C(4)−N(3)		1.344(5)	1.348(4)
C(6)−N(4)		1.308(5)	1.327(4)
C(1)−C(2)	1.398(2)	1.382(5)	1.385(4)
C(2)−C(3)	1.406(2)	1.425(6)	1.419(4)
C(4)−C(5)		1.382(6)	1.378(4)
C(5)−C(6)		1.420(5)	1.412(4)
C(1)−C(6)	1.508(2)[a]	1.516(6)	1.498(5)
C(3)−C(4)		1.506(6)	1.505(4)
Σ(N1)	358.6	353.5	359.1
Σ(N2)	359.3	358.4	359.0
Σ(N3)		352.8	358.4
Σ(N4)		360.0	358.2
C(2)−C(3)−C(4)−C(5)	48.6[a]	46.8	46.5
C(2)−C(1)−C(6)−C(5)		46.5	46.2
C(6)−C(1)−C(3)−C(4)	41.6[a]	41.0	40.1

[a]In this structure, because the cation lies on a crystallographic twofold axis, the atoms C(4), C(5), and C(6) should be replaced by the symmetry generated atoms C(1A), C(2A), and C(3A), which are their equivalents.

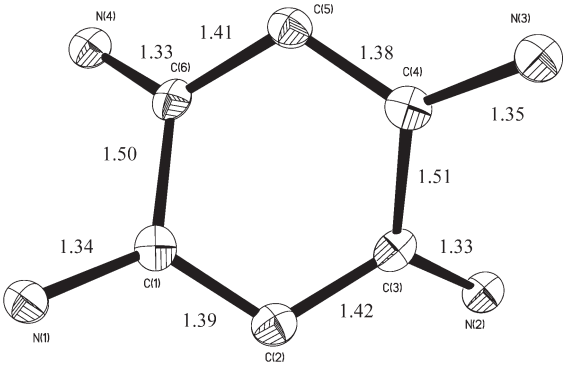

FIGURE 6. Core of $\mathbf{6}^{2+}$ (50% ellipsoids), showing the bond-length alternation (distances in Å) and the atom numbering scheme used.

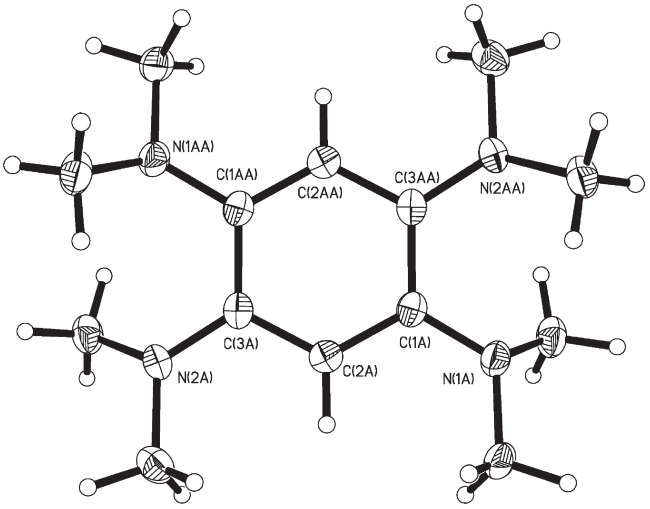

FIGURE 7. Crystallographic structure of cation **A** from polymorph I of [**1**][B{C$_6$H$_3$(CF$_3$)$_2$}$_4$].

radical species. Two different polymorphs of **2**[B{C$_6$H$_3$(CF$_3$)$_2$}$_4$] were crystallographically characterized; the first (polymorph I)

TABLE 5. Selected Bond Lengths (Å), Angles, and Torsion Angles (°) for the Radicals [2][B{$C_6H_3(CF_3)_2$}$_4$] and [4][B{$C_6H_3(CF_3)_2$}$_4$] (Σ(N1) = Sum of the Three Bonding Angles at N1, *etc.*)

	[2][B{$C_6H_3(CF_3)_2$}$_4$]						[4][B{$C_6H_3(CF_3)_2$}$_4$]	
	polymorph I				polymorph II			
independent molecule	A	B	C	D	E	F	A	B
N(1)−C(1)	1.383(3)	1.390(3)	1.384(3)	1.385(3)	1.376(3)	1.381(3)	1.400(4)	1.398(4)
C(1)−C(2)	1.385(3)	1.386(3)	1.384(3)	1.386(3)	1.390(3)	1.390(3)	1.379(5)	1.385(5)
C(2)−C(3)	1.402(3)	1.395(3)	1.401(3)	1.391(3)	1.389(3)	1.397(3)	1.409(5)	1.407(5)
C(3)−N(2)	1.369(3)	1.366(3)	1.367(3)	1.376(3)	1.376(3)	1.375(3)	1.368(4	1.371(4)
C(3)−C(1A)	1.445(3)	1.453(3)	1.447(3)	1.450(3)	1.448(3)	1.443(3)	1.450(4)	1.444(4)
ΣN (N1)	351.2	349.1	349.0	351.0	353.5	352.9	345.2	345.7
ΣN (N2)	355.9	354.6	356.2	353.5	352.3	352.9	357.3	355.8
C(2)−C(1)−C(3)−C(2)	5.3	5.4	6.3	6.4	6.4	5.7	4.0	3.7

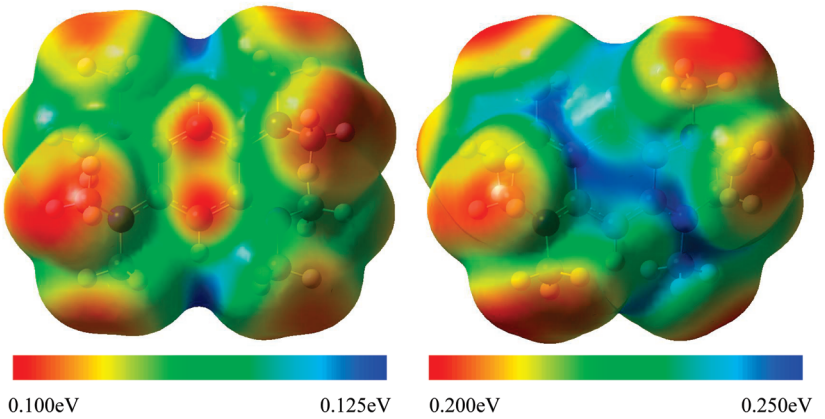

FIGURE 8. Computed electrostatic potential surfaces for $\mathbf{2}^+$ (left) and $\mathbf{2}^{2+}$ (right). Red = least positive, blue = most positive.

contains four half-molecules of $\mathbf{2}^+$ (and two complete anions) in the asymmetric unit, and the second (polymorph II) contains two half-molecules of $\mathbf{2}^+$ (and one complete anion) in the asymmetric unit, and there are thus 6 available values for each metric. The C−C distances range from 1.38 to 1.40 Å, except for the C(1)−C(3A) distance between the two halves of the system, which is in the range of 1.43−1.44 Å; the C−N distances go from 1.37 to 1.39 Å. It was predicted from the ESR spectrum of $\mathbf{2}^+$ that the nitrogen atoms were "close to planarity" and that there would be a close contact between the *endo*-methyl groups of neighboring NMe_2 moieties.[19] These inferences are supported by the crystal structures of $\mathbf{2}^+$, in which the sum of the angles at nitrogen varies from 349 to 356°, and the *endo*-methyl groups lie close to each other (carbon−carbon distances between 3.06 and 3.14 Å). The structure thus has aspects in common with those of both the neutral compounds and the dications; the planarity of the nitrogen atoms is characteristic of the latter, but the planarity of the central ring and the relatively short C(1)−C(3A) bond are reminiscent of the former. The shortness of this bond is probably due to the high contribution of the p-orbitals on C(1) and C(3) to the SOMO.[5] The structure of $\mathbf{4}^+$ has similar metrics to that of $\mathbf{2}^+$, though there is again some bond-length alternation in the C−C and C−N distances.

Computational Studies. Given that ion pairing does seem to be the cause of the observed potential inversion in the oxidation of these species, we sought further insight by means of a computational study. Computational studies on the effect of ion pairing on potential inversion appear to be limited to the reduction of cyclooctatetraene (COT) in the presence of $LiClO_4$ as electrolyte, in which tight ion pairs between the COT anions and lithium cations are important;[20] we have been unable to find any modeling studies on the ion pairing between analyte cations and electrolyte anions such as $[PF_6]^-$.

The geometries of both **1** and **2** (as computationally simple model compounds) were optimized in neutral, cationic, and dicationic forms, and then solvation was modeled using the PCM model. Electrostatic potential surfaces were then generated for the cations to locate the areas of maximum positive charge on the molecular surface and hence gain some indication of where any anions might be found. An anion was then manually placed there, and the geometry of the ion pair (or ion triplet for dication with two anions) optimized, and the solvation model applied again.

The potential surfaces (shown for $\mathbf{2}^+$ and $\mathbf{2}^{2+}$ in Figure 8) reveal that, for the monocation $\mathbf{2}^+$, the maximum positive charges are found on each side of the molecule, in the plane of the ring and next to the central hydrogen atoms. In contrast, for the monocation $\mathbf{1}^+$ and both dications $\mathbf{1}^{2+}$ and $\mathbf{2}^{2+}$, the maximum positive charges are above and below the center of the ring. Thus, two sites (side-on and face-on) were identified as possible locations for the anions, and we proceeded to optimize various ion pairs and triplets using these locations.

It was found that for the monocation $\mathbf{2}^+$ it was possible to optimize the geometry with an anion in either of the two

(19) Barth, T.; Neugebauer, F. A. *J. Org. Chem.* **1995**, *60*, 5401–5406.

(20) Fry, A. J. *Electroanalysis* **2006**, *18*, 391–398.

TABLE 6. Calculated Values of $\Delta_{disp}G$ (kcal mol^{-1}) for Disproportionation Reactions in Dichloromethane

	reaction	1		2	
	A	PF_6	ClO_4	PF_6	ClO_4
i	$2B^+ \rightarrow B^{2+} + B$	25.72		22.85	
ii	$2(B^+[A]^-) \rightarrow (B^{2+}[A]^-) + B + [A]^-$	−2.03	6.48	9.69[a]/−2.79[b]	7.92[a]/1.62[b]
iii	$2(B^+[A]^-) \rightarrow (B^{2+}2[A]^-) + B$	−4.68	6.55	6.08[a]/−6.40[b]	7.09[a]/0.79[b]
iv	$B^+[A]^- + B^+ \rightarrow (B^{2+}[A]^-) + B$	5.95	10.09	12.14[a]/5.90[b]	11.98[a]/8.83[b]
v	$2B^+ + [A]^- \rightarrow (B^{2+}[A]^-) + B$	13.93	13.70	14.59	16.04
vi	$2B^+ + 2[A]^- \rightarrow (B^{2+}2[A]^-) + B$	11.28	13.77	10.98	15.21
vii	$2(B^+[A]^-) \rightarrow B^{2+} + B + 2[A]^-$	9.76	18.50	17.95[a]/5.47[b]	14.73[a]/8.43[b]

[a]Side-on configuration of $\mathbf{2}^+$[A]. [b]Face-on configuration of $\mathbf{2}^+$[A].

TABLE 7. Calculated Values of $\Delta_{disp}G$ (kcal mol^{-1}) for Disproportionation Reactions in Acetonitrile

	reaction	1		2	
	A	PF_6	ClO_4	PF_6	ClO_4
i	$2B^+ \rightarrow B^{2+} + B$	19.93		16.8	
ii	$2(B^+[A]^-) \rightarrow (B^{2+}[A]^-) + B + [A]^-$	−6.97	1.45	5.08[a]/−8.06[b]	3.42[a]/−3.52[b]
iii	$2(B^+[A]^-) \rightarrow (B^{2+}2[A]^-) + B$	−4.01	7.32	7.04[a]/−6.10[b]	8.41[a]/1.47[b]
iv	$B^+[A]^- + B^+ \rightarrow (B^{2+}[A]^-) + B$	5.73	10.04	11.72[a]/5.15[b]	11.86[a]/8.39[b]
v	$2B^+ + [A]^- \rightarrow (B^{2+}[A]^-) + B$	18.43	18.63	18.36	20.30
vi	$2B^+ + 2[A]^- \rightarrow (B^{2+}2[A]^-) + B$	21.39	24.50	20.32	25.29
vii	$2(B^+[A]^-) \rightarrow B^{2+} + B + 2[A]^-$	−5.47	2.75	3.52[a]/−9.62[b]	−0.08[a]/−7.02[b]

[a]Side-on configuration of $\mathbf{2}^+$[A]. [b]Face-on configuration of $\mathbf{2}^+$[A].

locations, though the free energy of formation for the side-on position was more negative. In contrast, for $\mathbf{1}^+$, the system was only stable when the anion was in the face-on position; if the optimization was started from the side-on position, the anion migrated to the face-on location. For both the dications $\mathbf{1}^{2+}$ and $\mathbf{2}^{2+}$, stable ion pairs and triplets had one or two anions, respectively, in the face-on positions above one or both faces of the ring. Pleasingly, and implying that the calculations were giving the correct location of the anions, the crystal structure of [**2**][PF_6]$_2$ does indeed have the [PF_6]$^-$ anions located above and below the center of the ring (Figure 5).

Having calculated the free energy of formation for all species, we were then able to calculate $\Delta_{disp}G$ for various disproportionation reactions of $\mathbf{1}^+$ and $\mathbf{2}^+$ (Table 6). For the reaction $2B^+ \rightarrow B^{2+} + B$, $\Delta_{disp}G$ was found to be between 20 and 30 kcal mol^{-1}; in other words, disproportionation is highly disfavored.[21]

It is apparent from the data in Table 6 that only by allowing ion-pairing of all cations do the calculations imply that disproportionation *might* be favorable (reactions ii and iii, in which $\Delta_{disp}G$ is closest to 0). If there is no ion pairing, then $\Delta_{disp}G$ is on the order of 5−20 kcal mol^{-1} and the radical cation is stable with respect to disproportionation. The relative contribution of each of the reactions to the observed solution behavior will depend upon the concentrations of the species in solution, but overall, it is possible to say that ion pairing is necessary for potential inversion to occur for these molecules.

The data do not, however, definitively explain the observed experimental behavior. For example, similar values were obtained when acetonitrile was used as the solvent model (Table 7), whereas the experimental data show that in this solvent disproportionation occurs even in the absence of ion pairing. This is likely to be due to inadequate modeling of the highly directional acetonitrile−ion interactions by the solvent continuum model used; the experimental work of Geiger has shown these to be very strong,[16] and even a small fractional error in the calculation might cause the disagreement seen.

One qualitative observation that can be made is that the ion pairing in $\mathbf{1}^+$ and $\mathbf{2}^+$ is likely to be different; effectively, the presence of the fluorine atoms in **1** makes the 3 and 6 positions of the central ring "nonstick", and less effective ion pairing for **1** may be the reason why it has a greater value of ΔE than **2**.

Conclusions. The studies reported herein have shed light on the causes and the nature of the observed oxidations of 1,2,4,5-tetrakis(amino)benzenes. The original report by Staab included an electrochemical study in acetonitrile, under which conditions a single two-electron oxidation is seen,[2] and this has subsequently been attributed to the geometric changes observed on changing from neutral compound to dication. While the change in orbital energies associated with the geometry change is undoubtedly a factor in determining the electrochemical behavior, we have shown herein that the separation of the two oxidations is also both solvent- and electrolyte-dependent, and that these two factors must therefore also play a part in determining ΔE. Using the combination of a noncoordinating anion and a nonpolar solvent shows that in the system studied herein geometric change on its own is not sufficient to cause potential inversion, and that extra stabilization of the dication (by ion pairing or strong solvent−molecule interactions) is required for this phenomenon to be observed. This may well prove to be the case for a much wider variety of organic redox-active systems than just that reported here if the trends observed in the electrochemical studies of inorganic compounds with noncoordinating anions are followed by their organic counterparts.

Experimental Section

All reactions were carried out under a nitrogen atmosphere, using thoroughly dried solvents and glassware. **3**[7] and **4**[6]

(21) Macías-Ruvalcaba, N. A.; Evans, D. H. *J. Phys. Chem. B* **2005**, *109*, 14642–14647.

were synthesized according to the literature procedure, and **6** could be synthesized by the palladium-catalyzed methodology reported in the literature[10] or from **5** by the procedure outlined below. $[Bu_4N][B\{C_6H_3(CF_3)_2\}_4]$,[22] $Fc[B\{C_6H_3(CF_3)_2\}_4]$,[23] and $Fc[PF_6]$[24] were synthesized according to the literature procedures.

Synthesis of 1,2,4,5-Tetrakis(dimethylamino)-3,6-difluorobenzene 1: A round-bottomed flask was charged with lithium dimethylamide (26.7 mmol, 8.0 equiv relative to hexafluorobenzene, 40 mL of a 5% solution in hexanes). THF (20 mL) was added to give a 0.45 M solution of the amine, and the system was cooled to −20 °C. Hexafluorobenzene (0.62 g, 3.3 mmol) was added dropwise to give an orange solution, which was further stirred for 60 h. MeOH was added dropwise until decoloration of the reaction mixture was achieved (typically 3−5 drops), and stirring was continued for 5 min. The mixture was poured into a 20% aqueous KOH solution (20 cm^3) and extracted with diethyl ether (2 × 100 cm^3) and hexane (3 × 100 cm^3), washed with brine and water, and dried over $MgSO_4$. Evaporation of the solvent gave a mixture of white and orange solids, which were washed with small amounts of MeOH to leave 0.261 g of product as a white solid. Storage of the washings at −10 °C yielded another 0.400 g of product (total yield 0.661 g, 79%): ^{1}H NMR (301 MHz, $CDCl_3$) δ ppm 2.80 (t, J = 0.8 Hz, 24 H); ^{13}C NMR (76 MHz, $CDCl_3$) δ ppm 155.9 (d, J = 244.03 Hz), 134.8 (t, J = 9.23 Hz), 43.9 (br s); ^{19}F NMR (283 MHz, $CDCl_3$) δ ppm −135.1; MS (ESI) $[M + H]^+$ 287.20. Anal. Calcd for $C_{14}H_{24}F_2N_4$: C, 58.72; H, 8.45; N, 19.56. Found: C, 59.16; H, 8.69; N, 19.36.

Synthesis of 1,2,4,5-Tetrakis(dimethylamino)benzene 2: A Schlenk tube with a Young's tap was charged with freshly distilled DME (40 cm^3) and sodium (0.35 g, 15.28 mmol) under nitrogen. Biphenyl (1.62 g, 10.5 mmol) was added, and the mixture was vigorously stirred for 2 h to give a dark blue solution. **2** (0.409 g, 1.43 mmol) was added as a solid, and stirring was continued for 1 day. A few drops of an aqueous 20% HCl solution was added slowly and dropwise until decoloration of the mixture was achieved. The mixture was poured into 20% aqueous HCl solution (20.0 cm^3) and extracted with hexanes to remove biphenyl. The aqueous phase was basified with ammonia solution and extracted with diethyl ether (3 × 50 cm^3), washed with brine and then water, and dried over $MgSO_4$. Evaporation of the combined organic phases gave the product as an off-white solid, which was recrystallized from dichloromethane/MeOH to give the product as a white powder (0.298 g, 83%): ^{1}H NMR (300 MHz, C_6D_6) δ ppm 2.77 (s, 24 H), 6.68 (s, 2 H); ^{13}C NMR (101 MHz, C_6D_6) δ ppm 140.6, 109.7, 42.6; HRMS calcd for **2** 250.2152, found 250.2161. Anal. Calcd for $C_{14}H_{26}N_4$: C, 67.16; H, 10.47; N, 22.38. Found: C, 66.95; H, 10.56; N, 22.13.

Synthesis of 2$[PF_6]_2$: To a solution of 16 mg of **2** (0.064 mmol) in dry dichloromethane was added $Fc[PF_6]$ (43 mg, 0.128 mmol). Upon stirring, the solution became green and then deposited **2**$[PF_6]_2$ as a purple precipitate, which was isolated by filtration and washed with diethyl ether to give 18.1 mg (46 mmol, 72%) of product. Crystals for X-ray diffraction were grown by vapor diffusion of diethyl ether into an acetonitrile solution: MS (ESI) $[M]^+$ 250.22; HRMS calcd for $\mathbf{2}^+$ 250.2152, found 250.2150. Anal. Calcd for $C_{14}H_{26}F_{12}N_4P_2$: C, 31.12; H, 4.85; N, 10.37. Found: C, 31.48; H, 5.13; N, 10.21.

Synthesis of 2$[B\{C_6H_3(CF_3)_2\}_4]$: To a solution of **2** (31 mg, 0.124 mmol) in 10 mL of diethyl ether was added 135 mg (0.129 mmol) of $Fc[B\{C_6H_3(CF_3)_2\}_4]$[25] to give a bright green solution. The product was precipitated as a dark green powder by addition of excess hexane to give 120 mg (49%, 0.061 mmol). Crystals for X-ray diffraction were grown by layered diffusion of hexane into an ether solution: MS (ESI) $[M]^+$ 250.22; HRMS calcd for **2**$[B\{C_6H_3(CF_3)_2\}_4$ 1113.2800, found 1113.2782. Anal. Calcd for $C_{46}H_{34}BF_{24}N_4$: C, 49.61; H, 3.44; N, 5.03. Found: C, 49.70; H, 3.55; N, 5.00.

Synthesis of 4$[B\{C_6H_3(CF_3)_2\}_4]$: Seventeen milligrams (0.041 mmol) of **4** and 44 mg (0.042 mmol) of $Fc[B\{C_6H_3(CF_3)_2\}_4]$ were dissolved in a mixture of 6 mL of diethyl ether and 4 mL of CH_2Cl_2. A large excess of hexane was then carefully layered onto the top of the solution, and the solutions were allowed slowly to diffuse together to give **4**$[B\{C_6H_3(CF_3)_2\}_4]$ (45 mg, 86%) as large dark blue crystals: MS (ESI) $[M]^+$ 1273.42; HRMS calcd for **4**$[B\{C_6H_3(CF_3)_2\}_4]$ 1273.4058, found 1273.4066. Anal. Calcd for $C_{58}H_{54}BF_{24}N_4$: C, 54.69; H, 4.27; N, 4.40. Found: C, 54.53; H, 4.36; N, 4.67.

Synthesis of 4$[I_3][I_5]\cdot I_2$: Crystals of this compound were grown by adding solid iodine to a sample of **4** dissolved in $CDCl_3$ in an NMR tube. The sample was allowed to slowly evaporate, giving a few crystals of the product suitable for X-ray diffraction.

Synthesis of 1,2,4,5-Tetrakis(morpholin-1-yl)-3,6-difluorobenzene 5: A round-bottomed flask was charged with morpholine (2.813 g, 32.3 mmol, 8.0 equiv relative to hexafluorobenzene). THF (40 mL) was added, and the system was cooled to −20 °C. A solution of *n*-BuLi (20 mL, 1.6 M in hexanes, 32.0 mmol, 1.0 equiv relative to the amine) was added dropwise, and the mixture was stirred at −20 °C for 30 min. Hexafluorobenzene was added dropwise to give an orange solution, which was further stirred for 16 h while being allowed to reach room temperature, and the solution was then refluxed for 90 min. After cooling to room temperature, MeOH was added dropwise until decoloration of the reaction mixture was achieved (typically 3−5 drops) and no further color change was observed. Addition of a further 20 mL of MeOH caused the precipitation of the crude product as a white solid (leaving an orange supernatant), which was isolated by filtration and purified by being dissolved in CH_2Cl_2, filtered, and the solvent removed to give 0.705 g of product. The orange supernatant was evaporated to dryness and redissolved in CH_2Cl_2 to give a suspension which was treated with ultrasound for a few minutes. This was then filtered, and the gel-like solid was washed with 25 mL of hot CH_2Cl_2. The combined organic fractions were decolorized with charcoal and evaporated to dryness to give a further 0.073 g of product (63%): ^{1}H NMR (301 MHz, $CDCl_3$) δ ppm 3.79 (t, J = 5 Hz, 16H), 3.14 (t, J = 5 Hz, 16H); ^{13}C NMR (101 MHz, $CDCl_3$) δ ppm 51.50, 67.89, 133.57 (dd, J = 10.90, 7.79 Hz), 155.17 (dd, J = 246.01, 2.34 Hz); ^{19}F NMR (283 MHz, $CDCl_3$) δ ppm −133.29; MS (ESI) $[M + H]^+$ 455.25, $[M + Na]^+$ 477.23. Anal. Calcd for $C_{22}H_{32}F_2N_4O_4$: C, 58.14; H, 7.10; F, 8.36; N, 12.33. Found: C, 58.26; H, 7.17; F, 8.19; N, 12.20.

1,2,4,5-tetrakis(morpholin-1-yl)benzene **6** was prepared from **5** in 65% yield by a procedure analogous to that described above for the synthesis of **2** from **1**: ^{1}H NMR (400 MHz, $CDCl_3$) δ ppm 3.14 (t, J = 4.40 Hz, 16 H), 3.81 (t, J = 4.40 Hz, 16 H), 6.53 (s, 2 H); ^{13}C NMR (101 MHz, $CDCl_3$) δ ppm 50.29, 67.59, 109.28, 139.62; MS (ESI) $[M + H]^+$ 419.27. Anal. Calcd for $C_{22}H_{34}N_4O_4$: C, 63.13; H, 8.19; N, 13.39. Found: C, 62.83; H, 8.21; N, 12.95.

Synthesis of 6$[PF_6]_2$: To a solution of 0.051 g of **6** in 10 mL of CH_2Cl_2 was added 0.065 g of $Fc[PF_6]$. The suspension was stirred for 2 h, before the product was isolated by filtration as 52 mg (0.07 mmol, 60%) of microcrystalline green solid which was dried in vacuo: ^{1}H NMR (301 MHz, CD_3CN) δ ppm 3.80, 3.82 (each s, 8H), 5.95 (s, 2H); crystals for X-ray diffraction were grown by vapor diffusion of diethyl ether into an acetonitrile solution; MS (ESI) $[M]^+$ 418.26, $[M]^{2+}$ 209.13, $[M + PF_6]^+$

(22) Taube, R.; Wache, S. *J. Organomet. Chem.* **1992**, *428*, 431–442.
(23) Chávez, I.; Alvarez-Carena, A.; Molins, E.; Roig, A.; Maniukiewicz, W.; Arancibia, A.; Arancibia, V.; Brand, H.; Manuel Manríquez, J. *J. Organomet. Chem.* **2000**, *601*, 126–132.
(24) Connelly, N. G.; Geiger, W. E. *Chem. Rev.* **1996**, *96*, 877–910.
(25) Chavez, I.; Alvarez-Carena, A.; Molins, E.; Roig, A.; Maniukiewicz, W.; Arancibia, A.; Arancibia, V.; Brand, H.; Manriquez, J. M. *J. Organomet. Chem.* **2000**, *601*, 126–132.

563.22, $[M - C_4H_8NO + H]^+$ 348.19. Anal. Calcd for $C_{22}H_{34}F_{12}N_4O_4P_2$: C, 37.30; H, 4.84; N, 7.91. Found: C, 37.12; H, 4.83; N, 7.71.

EPR Spectroscopy: EPR spectra were recorded on a Bruker EMX Micro X-band spectrometer at room temperature using 1 mm thick quartz flat cells at the EPSRC Multi-Frequency cw EPR Service Centre at The University of Manchester. In situ EPR spectroelectrochemical experiments at room temperature were carried out in dichloromethane with 0.1 M $[Bu_4N][PF_6]$ (for **1**) or $[Bu_4N][B\{C_6H_3(CF_3)_2\}_4]$ (for **2**) as the supporting electrolyte, using platinum working and auxiliary electrodes and a Ag/AgCl reference electrode. The auxiliary and reference electrodes were both situated in the bulk solution above the cavity, and the Pt mesh working electrode was located in the flat part of the cell inside the cavity of the spectrometer. The potentiostat (Autolab, Type II) was controlled via a PC running General Purpose Electrochemical System software, version 4.9 (Eco Chemie BV, Utrecht). Simulations were performed using Bruker Win-EPR Simfonia software.

Electrochemistry: Electrochemical studies were carried out at room temperature (ca. 293 K) using an EG&G model 273A potentiostat linked to a computer using EG&G Model 270 Research Electrochemistry software in conjunction with a three-electrode cell. The auxiliary electrode was a platinum wire and the working electrode a glassy carbon disk (1.6 mm diameter). The reference electrode was an aqueous saturated calomel electrode separated from the test solution by a fine porosity frit and an agar bridge saturated with KCl. Under the conditions used, the reversible potential for the ferrocenium/ferrocene couple at 298 K is +0.38 V in acetonitrile and +0.46 V in CH_2Cl_2.[24] Solutions were 1.0×10^{-3} mol dm^{-3} in the compound and 0.1 mol dm^{-3} in supporting electrolyte. Voltammograms were simulated using DIGISIM version 3.03b (Bioanalytical Systems, Inc.); further details are available in the Supporting Information.

Crystal Structure Determinations: Diffraction intensities were collected on a Bruker SMART APEX CCD diffractometer, with graphite-monochromated Mo Kα (0.71073 Å) radiation. The data were corrected for absorption. The structures were solved by SHELXS-97, expanded by Fourier difference syntheses, and refined with the SHELXL-97 package incorporated into the SHELXTL crystallographic package.[26] The positions of the hydrogen atoms were calculated by assuming ideal geometries but not refined. All non-hydrogen atoms were refined with anisotropic thermal parameters by full-matrix least-squares procedures on F^2. Many of the details of the structural determinations are given in Table 8, and complete crystallographic details and tables of bond lengths and angles for all compounds are given in the Supporting Information. Many of the CF_3 groups of the $[B\{C_6H_3(CF_3)_2\}_4]$ anions showed rotational disorder, which was modeled using the approach of Müller.[27] The structure of **4**$[B\{C_6H_3(CF_3)_2\}_4]$ contains a single large residual electron density peak (of 2.052 e Å^{-3}) between two of the fluorine atoms of a CF_3 group. It was not possible to model this in a satisfactory fashion as there was no indication of the presence of two more peaks for the remaining fluorine atoms.

Computational Details. All calculations were performed with Gaussian 03 (revision B.04)[28] and used the popular B3LYP density functional.[29−31] All atoms were described by the all-electron 6-31G* basis set. Geometry optimizations were performed in the gas phase without either solvation or the imposition of symmetry, and an unsolvated $\Delta_f G$ for each species was then calculated according to the method of Ochterski.[34] Solvation was then applied using a dichloromethane (ε = 8.93) or acetonitrile (ε = 36.64) continuum solvation field, using the

TABLE 8. Crystallographic Details for All X-ray Structures

compound reference	**1**	**4**	**6**	**2**$[B\{C_6H_3(CF_3)_2\}_4]$ (polymorph I)	**2**$[B\{C_6H_3(CF_3)_2\}_4]$ (polymorph II)	**4**$[B\{C_6H_3(CF_3)_2\}_4]$	**2**$[PF_6]_2$·MeCN	**4**$[I_5][I_3]\cdot[I_2]$	**6**$[PF_6]_2$
chemical formula	$C_{14}H_{24}F_2N_4$	$C_{26}H_{42}N_4$	$C_{22}H_{34}N_4O_4$	$C_{46}H_{38}BF_{24}N_4$	$C_{46}H_{38}BF_{24}N_4$	$C_{58}H_{54}BF_{24}N_4$	$C_{16}H_{29}F_{12}N_5P_2$	$C_{26}H_{42}I_{10}N_4$	$C_{22}H_{34}F_{12}N_4O_4P_2$
formula mass	286.37	410.64	418.53	1113.61	1113.61	1273.86	581.38	1679.64	708.47
crystal system	monoclinic	monoclinic	monoclinic	monoclinic	triclinic	triclinic	orthorhombic	monoclinic	monoclinic
a/Å	5.6689(3)	12.5482(10)	7.990(3)	20.0324(10)	10.0811(14)	12.2176(4)	8.8766(10)	13.5646(5)	10.3234(12)
b/Å	16.6930(8)	8.0967(7)	6.322(2)	23.7621(14)	11.002(2)	12.7937(4)	12.1306(12)	17.3356(6)	16.922(2)
c/Å	8.1306(4)	13.0553(11)	20.989(8)	22.2774(12)	22.144(4)	21.1705(6)	22.447(3)	18.3183(7)	16.1800(18)
α/°	90.00	90.00	90.00	90.00	84.315(3)	97.433(2)	90.00	90.00	90.00
β/°	100.449(2)	117.338(4)	92.353(6)	115.616(2)	85.095(5)	96.910(2)	90.00	103.854(2)	94.011(7)
γ/°	90.00	90.00	90.00	90.00	78.110(5)	117.6170(10)	90.00	90.00	90.00
U/Å^3	756.65(7)	1178.26(17)	1059.2(7)	9562.0(9)	2386.3(7)	2845.60(15)	2417.0(5)	4182.2(3)	2819.7(6)
temperature/K	100(2)	100(2)	100(2)	100(2)	100(2)	100(2)	100(2)	100(2)	100(2)
space group	$P2(1)/n$	$P2_1/c$	$P2(1)/c$	$P2(1)/c$	$P\bar{1}$	$P\bar{1}$	*Pbcm*	$P2_1/c$	$P2(1)/c$
Z	2	2	2	8	2	2	4	4	4
no. of reflections measured	6158	19600	15332	88885	39675	44892	57228	9636	16907
no. of independent reflections	1739	3597	2451	22041	10872	12984	2871	9636	6086
R_{int}	0.0217	0.0337	0.0365	0.0555	0.0494	0.0280	0.0400	0.0000	0.0722
final R_1 values ($I > 2\sigma(I)$)	0.0367	0.0472	0.0662	0.0505	0.0475	0.0790	0.0317	0.0282	0.0572
final $wR(F^2)$ values ($I > 2\sigma(I)$)	0.0945	0.1188	0.2007	0.1316	0.0983	0.2247	0.0823	0.0595	0.1294
final R_1 values (all data)	0.0469	0.0628	0.0750	0.0869	0.0831	0.1046	0.0391	0.0407	0.1027
final $wR(F^2)$ values (all data)	0.1007	0.1268	0.2048	0.1542	0.1126	0.2554	0.0879	0.0628	0.1513

(26) Sheldrick, G. M. *Acta Crystallogr., Sect. A* **2008**, *64*, 112–122.
(27) Müller, P. *Cryst. Rev.* **2009**, *15*, 57–83.

default polarizable continuum model PCM[32,33] as implemented in G03 with radii optimized for the HF/6-31G* level of theory as recommended in the Gaussian 03 manual, which generates a Gibbs free energy of solvation. This was then added to the appropriate unsolvated $\Delta_f G$ value to yield the final solvated $\Delta_f G$; a table of these values for all species (Table S1) is available as part of the electronic Supporting Information. Attempts at geometry optimization with the application of solvation failed to converge for the ion pairs (hence the need to apply solvation after optimization), but comparison of these unconverged results with those obtained by retrospective application of the PCM continuum revealed no significant differences in either energy or geometry between the two methods.

Acknowledgment. We wish to thank the ESPRC for funding (C.J.A., R.C.D.C., M.F.H.). D.H.E. gratefully acknowledges support from the U.S. National Science Foundation, Grant No. CHE-0715375.

Note Added after ASAP Publication. Due to a calculation error, the values in Tables 6 and 7 and in the Supporting Information were incorrect in the version published ASAP on January 14, 2010; the corrected version was published on the Web February 12, 2010.

Supporting Information Available: Details of crystallographic structure determinations, computational details, electrochemical simulations, and NMR spectra. This material is available free of charge via the Internet at http://pubs.acs.org.

(28) Frisch, M. J.; Trucks, G. W.; Schlegel, H. B.; Scuseria, G. E.; Robb, M. A.; Cheeseman, J. R.; Montgomery J. A., Jr.; Vreven, T.; Kudin, K. N.; Burant, J. C.; Millam, J. M.; Iyengar, S. S.; Tomasi, J.; Barone, V.; Mennucci, B.; Cossi, M.; Scalmani, G.; Rega, N.; Petersson, G. A.; Nakatsuji, H.; Hada, M.; Ehara, M.; Toyota, K.; Fukuda, R.; Hasegawa, J.; Ishida, M.; Nakajima, T.; Honda, Y.; Kitao, O.; Nakai, H.; Klene, M.; Li, X.; Knox, J. E.; Hratchian, H. P.; Cross, J. B.; Adamo, C.; Jaramillo, J.; Gomperts, R.; Stratmann, R. E.; Yazyev, O.; Austin, A. J.; Cammi, R.; Pomelli, C.; Ochterski, J. W.; Ayala, P. Y.; Morokuma, K.; Voth, G. A.; Salvador, P.; Dannenberg, J. J.; Zakrzewski, V. G.; Dapprich, S.; Daniels, A. D.; Strain, M. C.; Farkas, O.; Malick, D. K.; Rabuck, A. D.; Raghavachari, K.; Foresman, J. B.; Ortiz, J. V.; Cui, Q.; Baboul, A. G.; Clifford, S.; Cioslowski, J.; Stefanov, B. B.; Liu, G.; Liashenko, A.; Piskorz, P.; Komaromi, I.; Martin, R. L.; Fox, D. J.; Keith, T.; Al-Laham, M. A.; Peng, C. Y.; Nanayakkara, A.; Challacombe, M.; Gill, P. M. W.; Johnson, B.; Chen, W.; Wong, M. W.; Gonzalez, C.; Pople, J. A. *Gaussian 03*, revision B.04; Gaussian, Inc.: Wallingford, CT, 2003.

(29) Lee, C. T.; Yang, W. T.; Parr, R. G. *Phys. Rev. B* **1988**, *37*, 785–789.

(30) Becke, A. D. *J. Chem. Phys.* **1993**, *98*, 5648–5652.

(31) Vosko, S. H.; Wilk, L.; Nusair, M. *Can. J. Phys.* **1980**, *58*, 1200–1211.

(32) Cossi, M.; Barone, V. *J. Chem. Phys.* **2001**, *115*, 4708–4717.

(33) Cossi, M.; Scalmani, G.; Rega, N.; Barone, V. *J. Chem. Phys.* **2002**, *117*, 43–54.

(34) Ochterski, J. W. *Thermochemistry in Gaussian*; Gaussian, Inc.: Wallingford, CT, 2000.